SUPERCONDUCTING REBALANCE ACCELERATION AND RATE SENSOR

R. Torti, M. Gerver, V. Gondhalekar, B. Maxwell
SatCon Technology Corporation
12 Emily Street
Cambridge, MA 02139

SUMMARY

The goal of this program is development of a high precision multisensor based on a high Tc superconducting proof mass. Design of a prototype is currently underway.

Key technical issues appear resolvable. High temperature superconductors have complicated, hysteretic flux dynamics but the forces on them can be linearly controlled for small displacements. Current data suggests that the forces on the superconductors decay over a short time frame and then stabilize, though very long term data is not available. The hysteretic force characteristics are substantial for large scale excursions, but do not appear to be an issue for the very small displacements required in this device. Sufficient forces can be exerted for non-contact suspension of a centimeter sized proof mass in a vacuum sealed, nitrogen jacket cryostat. High frequency capacitive sensing using stripline technology will yield adequate position resolution for 0.1 μg measurements at 100 Hz. Overall, a reasonable cost, but very high accuracy system is feasible with this technology. A summary of system parameters is given below.

Multisensor Performance	0.1 μg acceleration resolution 10^{-5} rad/sec^2 angular resolution
Pointing Mount Sensor Noise	1.6 x 10^{-5} A/hr drift 6 x 10^{-10} °/hr drift

INTRODUCTION

There is a need for improved acceleration and angular rate sensors for inertial guidance, vibration testing, and spacecraft pointing mounts. Current high precision rate gyros and gyroscopic accelerometers use spinning balls or wheels to increase their sensitivity. The complete systems with motors, sensors, and delicate balance are therefore very complicated and expensive.

SatCon has undertaken as a Phase II SBIR from NASA Langley Research Center (Contract NAS1-19938) the development of a combined rate and acceleration sensor ("multisensor") using high temperature superconductors and high resolution capacitive sensors that provide more accurate information, and are also less complex than current systems. These sensors may be operated as stand alone sensors or combined with a satellite mount for high accuracy pointing and tracking. We have focused on the feasibility of using a high temperature superconductor as the

proof mass and identifying the best sensor technology. Similar high accuracy sensors have been built using low temperature niobium superconductors, notably the superconducting gravimeter[1] and the NASA Grav-B gyro[2]. These systems, however, require expensive helium cooling, and do not provide angular and linear rates like the multi-sensor proposed here.

APPROACH

The concept behind the superconducting multisensor is very similar to a proof mass accelerometer. Proof mass accelerometers either measure the displacement of a spring restrained mass, and estimate the acceleration from knowledge of position and the spring constant or use feedback to maintain a constant position and use knowledge of actuator dynamics to estimate acceleration. Typically, high precision instruments use the rebalance scheme to minimize non-linearities in the spring restraint system, sensors, and actuators. The limited proof mass motion inherent in a rebalance system also allows more accurate position measurements to be made and improves performance. A suspended proof mass device, while more complex than spring restraint systems, has the further advantage of active control of the different stiffness and damping characteristics at different frequencies. This allows better vibration isolation from external disturbances.

A conceptual drawing of the sensor is shown in Figure 1. It consists of a cubical high temperature superconducting proof mass whose position is sensed and controlled by a set of co-located high frequency capacitive sensors and high T_c superconducting control coils fixed to the cryostat inner wall. The control coils are actuated based on sensor signals by an electronic control system to maintain a constant cube position. Knowledge of the mass dynamics of the cube and the actuator control signals allows three accelerations and three angular rates to be estimated. Though six sensors and actuators are sufficient to control the six degrees of freedom of the cube, twelve sets are shown to allow for averaging and redundancy. The cube, sensors, and control coils are contained in an evacuated cryostat with a cryogenically cooled jacket. The sensors and actuators are fixed to the cryostat and the cube is freely suspended. For use in ground based systems, a separate gravity lift coil would be placed in the outer cryogenic. The sensor and control electronics would be external to the cryogen and pass signals through hermetically sealed leads. The entire system excluding electronics is roughly softball-sized, about 8 cm in diameter.

The device has several features that should give it high accuracy. First, the high frequency capacitive sensors offer position sensitivities of 10^{-3} angstroms/$\sqrt{Hz}$. Second, the proof mass, sensors and coils are cooled to 77 degrees Kelvin. This reduces the thermal noise in the system. Third, the use of a superconducting proof mass and actuator generates very little heat in the system, reducing thermal gradients which would degrade precision. Overall, the device could have stand alone resolution of 0.1 μg acceleration and 10^{-5} rad/sec^2 angular acceleration and would drift 75 angstroms and 5 x 10^{-5} degrees in one hour due to sensor noise. These numbers are based on a bandwidth of 100 Hz, the use of capacitive position sensors with noise of 1.5 x 10^{-3}Å/$\sqrt{Hz}$ and a cube of diameter 2 cm. The drift is assumed to be a random walk, with time step $(10^{-2}/2\pi)$ seconds, and spatial step equal to the sensor noise at 100 Hz. Any systematic (non random) drift would be in addition to drift from sensor noise.

A selection of materials and their properties is shown in Table 1[3]. The YBaCuO compounds combine acceptable transition temperature with repeatable, well known, fabrication processes, and non-toxicity. The current proof mass design is based upon the YBa_2CuO_x compound. It is readily available, and the processed proof mass cube can be made to order by vendors.

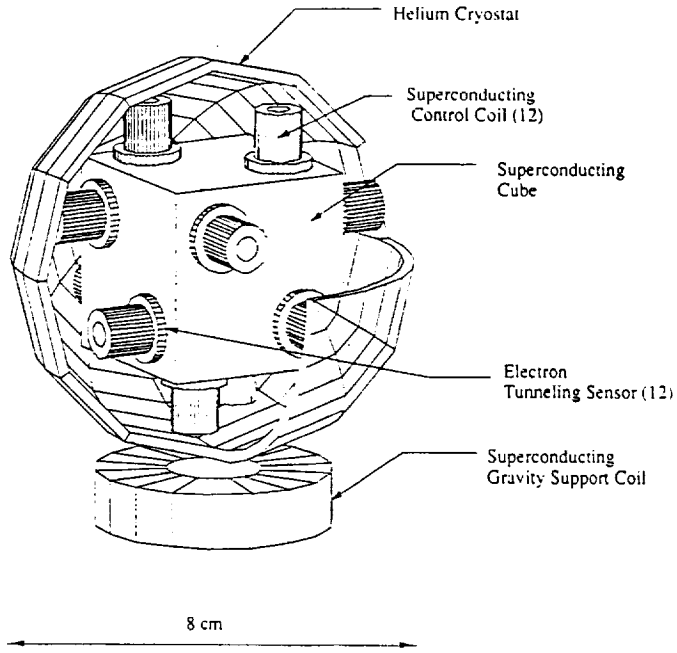

Figure 1. Superconducting Multisensor Concept

Table 1.

Material System	**T_c(K)**	**Coherence Length (Å)**	**Known Synthesis Properties**
Isotropic			
$(BA,K)BiO_3$	20-30	43	Difficult (Hygroscopic)
$YBa_2Cu_3O_x$	60-90	31	Most well Known
Tl/A/Cu/O	90-120	16-30	Toxic, Not Well Known
$(Nd,Ce)_2CuO_{4+x}$	22-30	70	Not Well Known
Bi-Sr-Pb-Ca-Cu-O	88-110	30-40	Relatively Well Known
Bi-Sr-Sb-Ca-Cu-O	90-132	---	Unknown
Most Anisotropic			

FORCES ON SUPERCONDUCTORS

For practical applications of high temperature superconductors, the area of greatest research is the phenomenology of forces on high T_c materials. The global force characteristics of these materials are very complicated and depend on temperature, field, chemical composition, and fabrication. The repulsive force mechanism arises from supercurrents that arise in the bulk superconductor in response to external magnetic fields. Since these currents are persistent and act to counter externally imposed fields, a persistent repulsive force is generated.

Macroscopically, the force is described by an integral of the Lorentz force between the supercurrents and externally applied field over the volume of the superconductor:

$$F = \iiint J_c \times B_r \, dV \qquad \text{Eq. 1}$$

Analytical and/or finite element solutions to this equation can be used to estimate the repulsive forces. Rao[4] presents experimental verification of finite element analyses of the repulsive forces between a magnet and HT_c superconductor.

An analytical approximation was made for the geometry of interest, as shown in Figure 2.

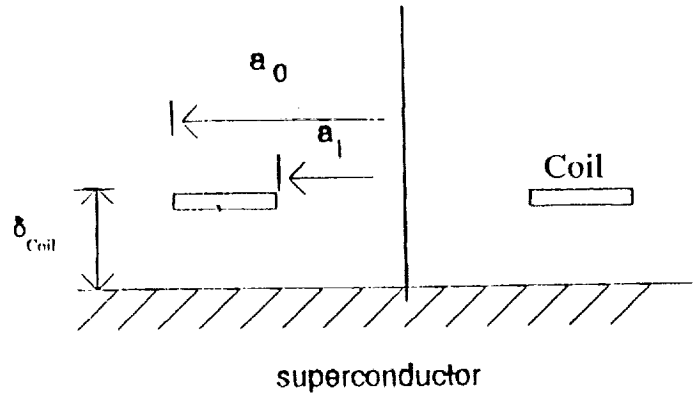

Figure 2. Coil Geometry

In the gap, if $\delta_{coil} << a_0 - a_i$, the magnetization H is approximately:

$$H = \frac{I}{a_0 - a_i} \qquad \text{Eq. 2}$$

$$B = \frac{I\mu_0}{(a_0 - a_8)} \qquad \text{Eq. 3}$$

$$\text{Field energy} = \int dV\ B \cdot H = \frac{I^2 \mu_0\ \delta_{coil}}{2(a_0 - a_i)}\ \pi(a_0 + a_i) \qquad \text{Eq. 4}$$

$$F = \frac{\pi}{2} I^2 \mu_0 \frac{(a_0 + a_i)}{(a_0 - a_i)} \qquad \text{Eq. 5}$$

The force can be calculated from the differential of the field energy $\int dV\ B \bullet H$, as above. The net force can be made linear in I by running a bias current, with opposing coils in series, as usual in magnetic bearings.

An issue of concern is in the effect of flux pinning on the magnet forces. High temperature superconductors have the capacity to trap (or "pin") flux in their interiors if it is present when the material makes the transition to the superconducting state. This phenomena allows a permanent magnet to stably suspend below an HT_c sample and is also responsible for the range of stable suspension points, with little spring restraint between them.

This behavior is not desired for an instrument such as this, where a consistent force behavior is needed for accurate performance. Fortunately, work at Argonne National Laboratory[5], and at the Institute of Chemical Physics Academy of Sciences of the USSR[6] shows that this behavior disappears if alternating fields exist in the sample. This opens up the possibility of using a small field dither or control forces generated in response to environmental vibration to avoid these effects. Also, the proof mass motion under rebalance control will be so small that any hysteretic effects will be effectively linearized.

SENSORS

The key aspect of the superconducting multi-sensor is high resolution position sensors. Sensors derived from two technical developments were considered: electron tunneling and near microwave frequency driven capacitive sensors.

Electron Tunneling Sensors

Recent developments in the application of electron tunneling phenomena to instrumentation capable of producing sub-angstrom topographical maps of the surfaces have opened up many exciting new possibilities in imaging and sensing.

However, while electron tunneling sensors possess extremely high position sensitivities independent of sensor size and without complicated electronics, they have several disadvantages in this application. They are subject to mechanical shock and are too sensitive to surface topography.

Since the tip must protrude beyond the mechanical guard surface, an external shock which overwhelms the electronic stiffness of the control system may force the superconducting proof mass into a tip with possible tip and surface damage and an apparent acceleration renormalization.

Furthermore, since the tip is extremely sensitive to separation and does little spatial averaging, lateral motion of the proof mass will result in a trace of atomic-sized surface features as in the scanning microscope. The device would then be mapping the proof mass surface features instead of measuring accelerations and rates.

Capacitive Sensors

Capacitive sensors are widely used to sense displacement. They are mechanically simple, robust, and can be used to make fairly accurate position measurements. Because they sense the capacitance of a finite area, they can be designed insensitive to surface topology.

Operation utilizes displacement currents across gaps between capacitively coupled surfaces. Typically, a constant current sine wave is imposed on a flat sensor plate set near the target. The voltage and current are related by:

$$I = V \omega C$$

where C is the capacitance of the sensor to the target. This capacitance has the form:

$$C = \varepsilon A/d$$

where ε is the permittivity of the space between them, A is the sensor area, and d the separation. Since C is inversely proportional to gap, for a constant current, voltage is directly proportional to gap:

$$V = I\, d/(\varepsilon A \omega)$$

Practical drive circuits utilize an oscillator which drives a constant current into the measured capacitance. To reduce the effects of stray capacitance, the signal is co-axially guarded between the electronics and the sensor head. A feedback loop forces the guard voltage to be the same as the drive voltage, thus eliminating the effect of stray capacitances. The guard voltage is then proportional to the gap distance, and is demodulated and filtered to produce a linear output signal.

Commercially available sensors come in various sizes and ranges, with larger sensors being used for longer ranges (so the capacitances stay roughly the same). The typical dynamic range of 1000 gives a commercial sensor with 0.066" diameter a range of 0.001" and about 25 nm resolution which is not in the same league as electron tunneling sensors.

In a conventional electromagnetic sensor, circuit shot noise may be expected to dominate at frequencies above 1 kHz. We can estimate resolution limitations from shot noise in a capacitive sensor. The current is:

$$I = V\, \omega C = V\, \omega\, \varepsilon\, A/d$$

where d is the plate separation, ω is oscillator drive frequency, and A is the plate area.

If limited by shot noise, the position sensitivity limit is:

$$\delta d = d\sqrt{(2e/I)}.$$

δd can be reduced, however, by increasing the drive frequency. In standard guarded sensor circuits, this is not done because the guard loop must respond at a much higher frequency, several megahertz typically. Increasing the oscillator frequency has its limits because it is difficult to increase the guard frequency with standard electronics packaging. The stripline surface mount circuit developed by RCA for a capacitive video disc reader operates at 915 MHz. It uses high speed bi-polar semiconductors and placement of the circuits very near the sensor plate (within a few centimeters). Moreover, guarding is not required since the capacitance is compensated so that the device operates in a limited region on the slope of the tuning curve.

This technology has been demonstrated in a high precision seismometer at JPL[7]. The position sensitivity of the sensor is about 0.0015 A/√Hz; not quite as good as tunneling tips but in a package that is much more robust and reliable than electron tunneling sensors and is compatible with the acceleration resolution anticipated with the superconducting multisensor.
In order to evaluate the suitability of the proposed high frequency electronics as for sensing, we have acquired a commercial RCA video and are modifying essential components into suitable test electronics.

A re-construction of the resonator circuit is shown in Figure 3. The resonator section is driven from the oscillator shown at the lower left side. Variations in capacitance result in movement along the slope of the tuning curve and are detected through D2 and buffered by Q1 to produce the detector output. Additionally, this signal is coupled into an AFC circuit which in turn maintains the operating point within desired limits.

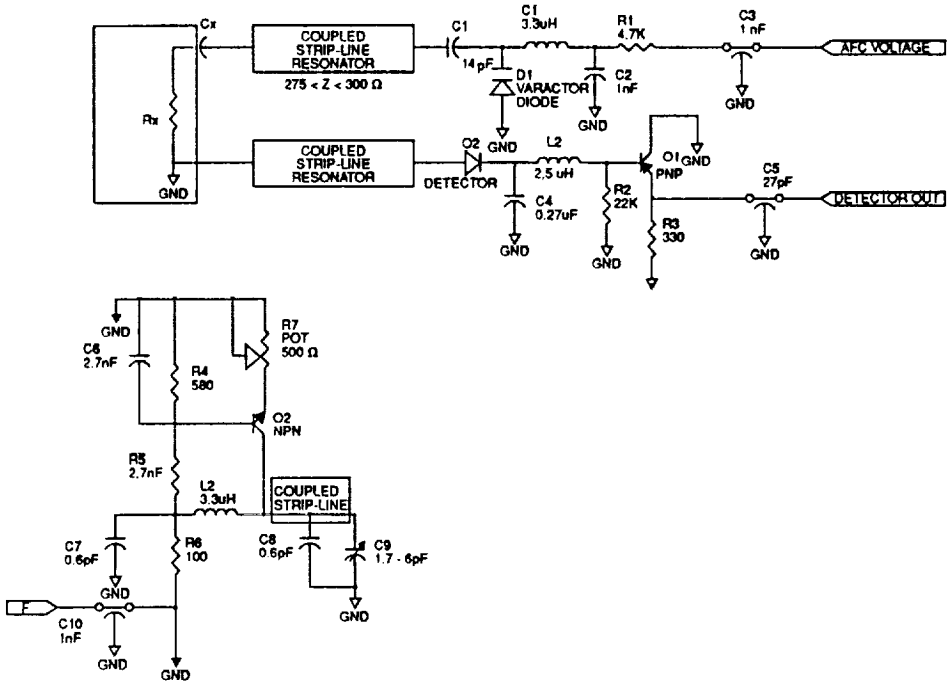

Figure 3. Re-construction of Resonator for RCA VideoDisc Player.

SYSTEM CONFIGURATION AND SIZING

This section explains the rationale behind the system configuration and sizing. As discussed earlier, the underlying goal was to design a high performance combined acceleration and angular rate sensor that is less complex and expensive than current inertial instruments. To this end, high temperature superconducting materials were selected instead of low temperature materials because liquid nitrogen cooling is much simpler and cheaper. Though the high temperature materials have less well understood and more complex flux dynamics, these effects are effectively eliminated by a control loop. The position of the suspended body is maintained so closely that the hysteretic features cannot be seen.

Proof Mass Shape

Since the instrument was conceived as a six degree of freedom device, it follows that the proof mass must have six degrees of freedom. This further implies a completely suspended and controlled proof mass. Acceleration sensitivity comes from sensing translations of the proof mass center and rotation sensitivity from sensing rotations about the center. The simplest practical shape that allows this is the cube. By sensing the distance between strategically placed sensors and the proof mass, it is possible to determine the translations and rotations with six sensors.

Sizing Issues

Initial sizing estimates were driven by observations of similar instruments. Superconducting gravimeters are sensitive two axis accelerometers that use a 1 inch niobium sphere suspended in superfluid liquid helium with superconducting control coils, capacitive position sensors, and rebalance control. The NASA Grav-B gyro, meant to be the most accurate gyro ever, with less than 10^{-10} degrees/hr drift rate uses a similar sized quartz sphere coated with niobium, suspended with capacitive sensors, and controlled by electrostatic actuators.

The sizing of these instruments and the superconducting multisensor is driven by several factors: resolution, cooling, suspension, and cost among others. Fundamental sensitivity is usually increased with increased mass and size. For a given resolution sensor, longer moment arms or greater proof mass imply smaller angular rate changes or result in larger control coil rebalance currents. Other issues such as mechanical rigidity and thermal drift and thermal gradients have generally limited this trend since larger systems are more likely to have undesirable structural resonances or thermal gradients.

In this superconducting sensor, there were additional factors involved in determining overall system size: superconductor fabrication considerations, suspension control, and cooling.

Fabrication

Structural integrity of the brittle high T_c materials precludes fabrication of cubical shapes much greater than a 2 cm face.

Control

From a control aspect, suspension of the proof mass in a vacuum avoids coupling to and damping by a gaseous medium and corruption of sensor signals. Vacuum operation also minimizes the exposure of the surfaces to humidity and gaseous corrosives.

Cooling

For operation at 77° K in a vacuum, the cooldown time becomes an issue. This places a constraint on proof mass size since heat content goes with volume while radiative cooling goes with area. The cooling from combined radiational and conduction loss can be expressed by:

$$\dot{Q} = \frac{dT}{dt} C_v m = (T_i - T_o) R 4\pi K + \sigma \epsilon A (T_i^4 + T_o^4) \qquad \text{Eq. 6}$$

Here A_i is the surface area of the proof mass, σ the Stefan-Boltzmann constant, ε the emissivity, m the proof mass, T_i the interior temperature, T_e the external temperature, a and b the temperature dependent coefficients of a specific heat, K the thermal conductivity of the gaseous medium, $C_v = a + b \bullet T$, and R the effective radial separation to the chamber walls. For this analysis, it is assumed that the emissivity, ε, is the same for the proof mass and the surrounding inner wall of the nitrogen jacket.

Cooldown time can be calculated by solving for dt and integrating over the temperature range. Results are displayed in Figure 4.

The following values were used:
m = 51g
ε = 0.96 (approx. black body, typical for roughened metals)
a = 30 J/kg - °K
b = 1.8 J/kg - $°K^2$
K = 0.04 to 0.12 watts/(sec•m•°C)
R = 0.02 m

A cube 2 cm on a face requires cooling in a vacuum and requires a barely acceptable 12 hours to drop from room temperature to about 80° K. However, the simple expedient of back-filling the chamber with a dry gas to aid in heat transfer, then proceeding with evacuation once the proof mass is at temperature, drastically reduces cooldown time.

Actuator Coils

The heat analysis also gives another important result. Because there is no convective heat transfer, and no conduction from the suspended mass, only a limited amount of heat can be generated in the cryostat and maintain temperature below transition. In this case, with the dimensions as above, approximately 4 mW can be removed by radiation.

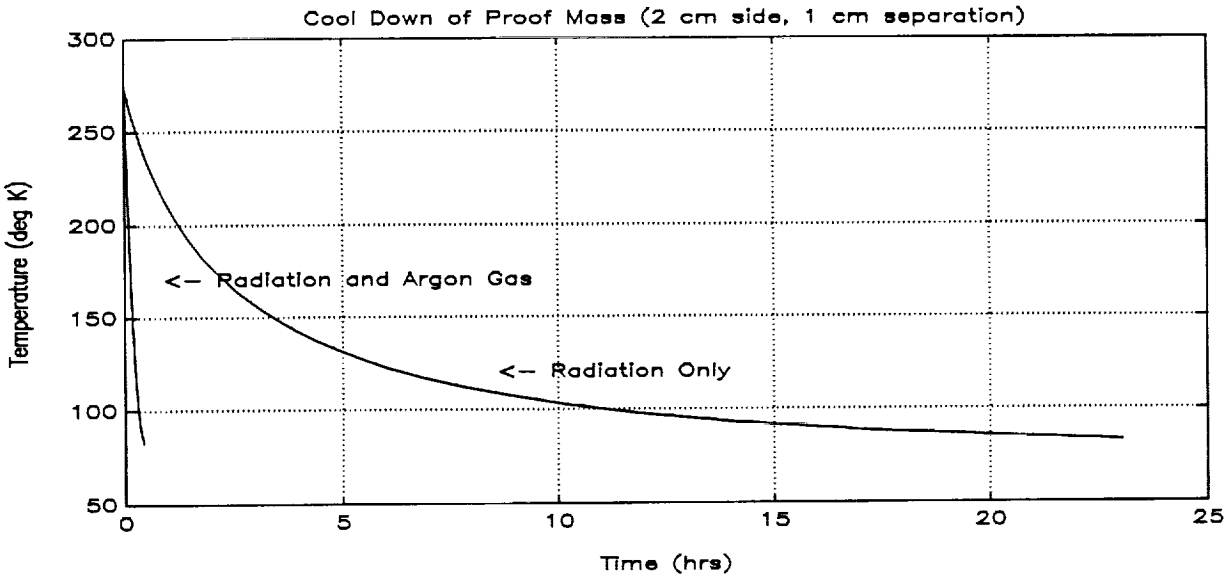

Figure 4. Proof Mass Cooldown.

This limited power dissipation puts serious constraints on the system. Copper control coils could only produce 0.1 g of the control force within this limitation if all heat is removed radiatively. Use of superconducting control coils obviates this with about the same volume as copper coils. We can obtain an acceleration of 0.8 g using two coils on a side, each with a current of 180 amp-turns, 1 cm outer diameter, and a square cross sectional of 2 mm a side. This fits easily within the available space and with the proof mass size.

Gravity Suspension

Operation in a ground based system requires a static force to offset gravity. This can be provided either with coils or permanent magnets.

High strength permanent magnets are clearly capable of suspending the proof mass with the obvious advantage of operating without power. However, the magnet material is long term unstable to a few percent and so a change in magnet field would change the vertical equilibrium position of the proof mass, which would be interpreted as a static acceleration.

Additionally, because of the flux pinning effects, HT_c materials can have different force characteristics depending on their magnetization state when the superconductor passes through its transition temperature. As shown by Chu[8], the force between an HT_c superconductor and a magnet is different for the field cooled, and the zero field cooled cases, with the zero field cooled case having more force.

These problems can be overcome, however, with the use of a coil to provide the static lifting force. A larger sized superconducting coil can be placed in the liquid nitrogen jacket and driven with a current control loop to generate the required support field, but with much better long term stability. This also allows the proof mass to be zero field cooled for better performance.

Mechanical Structure and Integration

The current mechanical structure of the system will be unlike the concept illustrated earlier. The cryostat will be a three chamber cylindrical shaped structure made of stainless steel with an insulating nitrogen jacket, cryostat, and inner chamber. The top cap will be removable and contain the entire active apparatus: proof mass, sensor electrode supports, support positioning, coils and include provision for electrical feedthrus and vacuum pumping. Speed sensor and control electronics will be placed external to the outer cryostat and operate at room temperature with RF

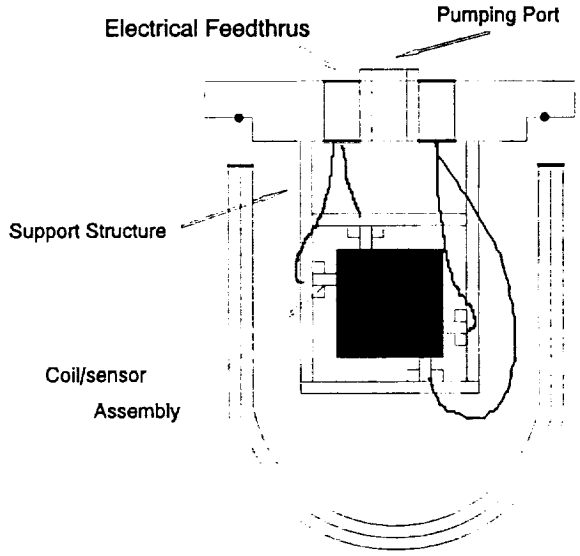

Figure 5 Current Mechanical Structure Including Cryostat, Proof Mass, Sensor Electrodes, Coils, and Feedthrus.

feedthrus in the cap. The cryostat design will be done in conjunction with the vendor.

CONTROL SYSTEM ANALYSIS AND DESIGN

The operation of the Superconducting MultiSensor is based on measurement of force and moments required to restore the proof mass, i.e., the superconducting cube, to a center zero orientation. A force/moment rebalance controller with a displacement feedback is the basis for achieving this aim. The principle is best illustrated with a single degree of freedom force rebalance system as shown in Figure 6. The block diagram in the figure shows a position feedback loop around a proof mass. F_{ext} is the external force acting on the proof mass. The force rebalance loop utilizes the position feedback signal to cancel out the external force F_{ext} with a force F_c thus forcing back the proof mass to a center zero position. The transfer function F_c/F_{ext} with reference to Figure 6 is

$$F_c/F_{ext} = C(s)*P(s)*H(s)/(1 + C(s)*P(s)*H(s)) \qquad \text{Eq. 7}$$

where s is the Laplace operator.

The force error $F_e = F_{ext} - F_c$ is a measure of the difference between the external force and the control force. The transfer function for the error F_e is:

$$F_e = 1/(1 + C(s)*P(s)*H(s)) \qquad \text{Eq. 8}$$

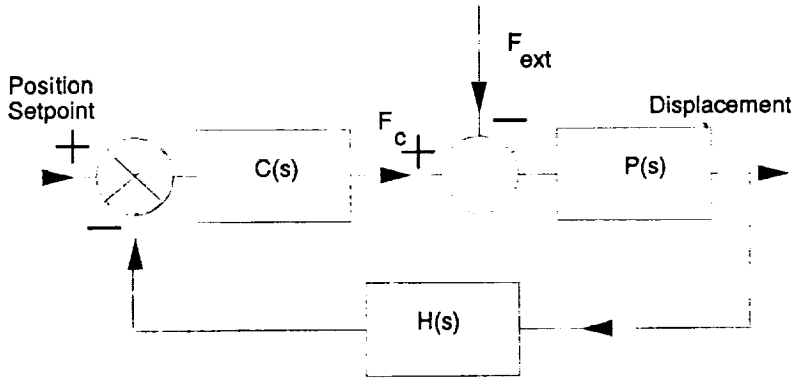

Figure 6 Single Degree Of Freedom Force Rebalance

Ideally, the steady state error F_e should be zero to give an accurate measure of the external force given that the control force F_c is known.

With normal proof mass based accelerometers, the proof mass "m" is supported on a cantilever with a finite stiffness coefficient "k" and a small damping coefficient "c". Hence the transfer function P(s) relating applied force F to displacement D is

$$P(s) = D/F = 1/(m*s^2 + c*s + k) \qquad \text{Eq. 9}$$

The source of stiffness or damping action on the S/C Multi sensor proof mass can potentially arise due to a flux pinning effect within the superconducting material and viscous damping introduced by the gases surrounding the proof mass. However, if the control forces are small; that is, if the control currents and the corresponding magnetic flux excursions experienced by the superconducting material are small, then the flux pinning will be minimal. Moreover the superconducting multisensor is housed in an evacuated dewar thus eliminating viscous damping. Under these conditions both the coefficients "k" and "c" will be zero. Eq. 8 becomes:

$$F_e = m*s^2/(m*s^2 + C(s)) \qquad \text{Eq. 10}$$

This will assure a zero steady state error. The transfer function is:

$$F_c/F_{ext} = C(s)/(m*s^2 + C(s)) \qquad \text{Eq. 11}$$

which gives the frequency response of the measurement. The form of the compensator C(s) will determine this frequency response.

The multisensor has six degrees of freedom: namely x,y,z translation and θ_x, θ_y, and θ_z rotations as shown in Figure 7. The actuator coils and capacitive sensors are collocated. There can be one or two sensors and actuators reacting against each face of the cube shaped proof mass (six or twelve total). Each actuator coil and sensor pair is located on a diagonal of the face as shown in Figure 7.

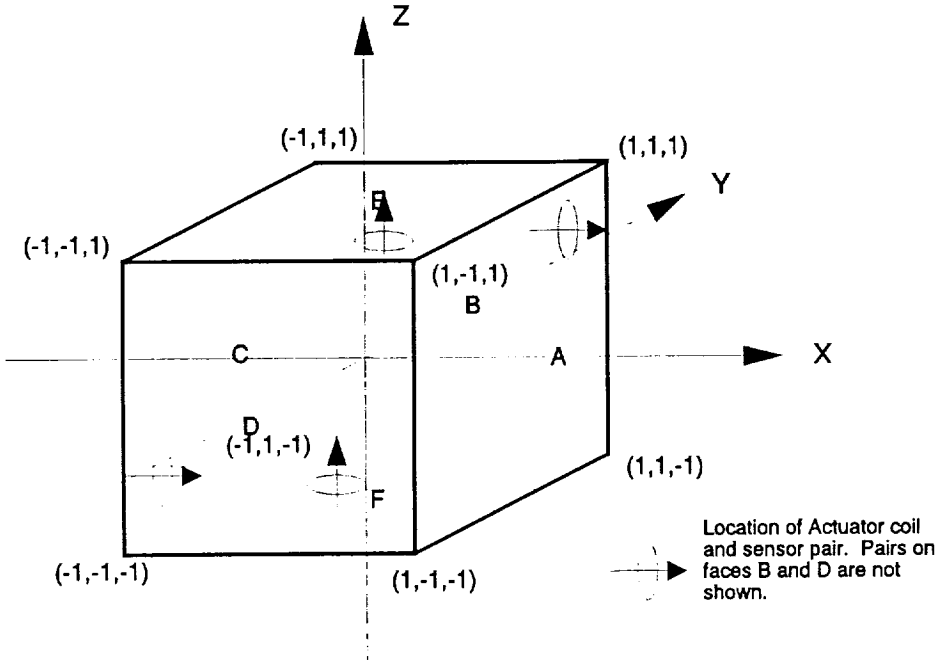

Figure 7 Sensor And Actuator Location Nomenclature

By virtue of the location of the actuator coil/sensor pair, each pair can generate a force along one translational axis and a moment around two rotational axes. If the forces generated by the actuator coils are defined by a vector

$$F_{act} = [F_a, F_b, F_c, F_d, F_e, F_f]^{-1}$$

then a transformation can be found which relates F_{act} the forces and moments

$$FM = [F_x, F_y, F_z, M_x, M_y, M_z]^{-1}$$

where the forces are defined along the translational axis and the moments are defined around these axes; i.e.,

$$FM = [T]*F_{act}$$

As the sensors are collocated with the actuator coils, the displacements measurement "d" at each sensor can be transformed to translations and rotations using the same matrix [T], i.e.,

$$[X, Y, Z, \theta_x, \theta_y, \theta_z]^{-1} = [T][d_a, d_b, d_c, d_d, d_e, d_f]^{-1}$$

The coefficients k_{n1}, k_{n0}, k_{d1} and k_{d0} of the compensation C(s) can now be tailored to meet the frequency response requirements of the sensor system. The numerator and denominator roots or the zeros and poles of the compensation C(s) were designed to be at 503 rad/sec and 3745 rad/sec respectively. The frequency response with this compensation scheme has an overshoot of 4db at 107 Hz with a 3db point attenuation at about 200 Hz. An improved performance can be achieved using a more complex controller.

REFERENCES

1. M. Browne, "Scientists Clock The Ticking Of The Earth's Core", New York Times, Page C1, March 31, 1992.

2. "Testing Einstein With Orbiting Gyroscopes", Stanford University Publication Services, NASA Astrophysics Division, 1990.

3. L. Rochemont et al, "Recent Progress Towards Developing a High Field, High-Tc Superconducting Magnet for Magnetic Suspension and Balance Systems", International Symposium on Magnetic Suspension Technology, August 19-23, 1991.

4. D. Rao, "Effect of Flux Penetration on the Load Bearing Capacity of Superconducting Bearings", International Symposium on Magnetic Suspension Technology, Langley Research Center, Hampton, VA August 19-23, 1992.

5. J. Hull, and M. Mulcahy, "Phenomenology of Forces Acting Between Magnets and Superconductors", pre-print.

6. A. Terentiev, and A. Kuznetsov, "Levitation of $YBa_2Cu_3O_7$ Superconductor In A Variable Magnetic Field". International Symposium on Magnetic Suspension Technology, Langley VA, August 19-23, 1992.

7. T. Van Zandt, T. Kenny, W. Kaiser, "Novel Position Sensor Technologies for Micro Accelerometers", Jet Propulsion Laboratory, Pasadena, CA

8. Chu, et al, "Hybrid Superconducting Magnetic Bearing For High Speed Drives", International Symposium on Magnetic Suspension Technology, Langley Research Center, Hampton VA, August 19-23, 1991.

omit

Session 9a (i) – Vibration Isolation

Chairman: Douglas B. Price
NASA Langley Research Center